ACADEMIC PRESS

Available online at www.sciencedirect.com

SCIENCE DIRECT®

Journal of Computational Physics 184 (2003) 366–380

JOURNAL OF COMPUTATIONAL PHYSICS

www.elsevier.com/locate/jcp

A further study of numerical errors in large-eddy simulations

Fotini Katopodes Chow [a,*], Parviz Moin [b]

[a] *Environmental Fluid Mechanics Laboratory, Department of Civil and Environmental Engineering, Stanford University, Stanford, CA 94305, USA*

[b] *Department of Mechanical Engineering, Stanford University, Stanford, CA 94305, USA*

Received 13 September 2001; received in revised form 24 June 2002; accepted 30 September 2002

Abstract

Numerical errors in large-eddy simulations (LES) arise from aliasing and discretization errors, and errors in the subfilter-scale (SFS) turbulence model. Using a direct numerical simulation (DNS) dataset of stably stratified shear flow to perform a priori tests, we compare the numerical error from several finite difference schemes to the magnitude of the SFS force. This is an extension of Ghosal's analysis [J. Comput. Phys. 125 (1996) 187] to realistic flow fields. By evaluating different grid resolutions as well as different filter–grid ratios, we provide guidelines for LES: for a second-order finite difference scheme, a filter–grid ratio of at least four is desired; for a sixth-order Padé scheme, a filter–grid ratio of two is sufficient.

© 2002 Elsevier Science B.V. All rights reserved.

Keywords: LES; Large-eddy simulation; Numerical error analysis; Turbulence

1. Introduction

Large-eddy simulation (LES) has become an increasingly used method for predicting turbulent flows. However, LES and direct numerical simulation (DNS) both suffer from discretization and aliasing errors that depend on the numerical schemes used. Because of computational limits, LES has an additional source of error owing to the fact that the velocity field is not fully resolved. The Navier–Stokes equations are filtered, and the effect of subfilter-scale (SFS) motions is modeled. Thus numerical errors in LES result from aliasing and discretization errors, as well as from errors in the SFS model.

Much of the current research in LES is focused on the development of improved SFS models, without reference to perhaps more significant, numerical errors that are present. However, as LES is applied to more complex problems, it will become even more important to understand errors inherent in the numerical schemes used, especially if we hope to create accurate forecast models. While a spectral, dealiased code may be able to avoid aliasing and finite difference errors (though not SFS errors), virtually all turbulence

* Corresponding author.
E-mail addresses: katopodes@stanfordalumni.org (F.K. Chow), moin@stanford.edu (P. Moin).

0021-9991/02/$ - see front matter © 2002 Elsevier Science B.V. All rights reserved.
PII: S0021-9991(02)00020-7

calculations in complex domains are carried out with finite differences. When finite differences schemes are used, truncation errors as well as the formulation used for nonlinear terms of the Navier–Stokes equations have been shown to be important for numerical stability and accuracy [5]. Furthermore, assessment of truncation and aliasing errors is crucial for ensuring that the contribution of the SFS forcing is not dominated by numerical errors.

A systematic analysis of these numerical errors is difficult because of nonlinear interactions between them. The traditional linearized analysis of errors for partial differential equations is therefore not adequate. Ghosal [3] was able to draw important conclusions by using statistical analysis to derive errors in LES from a random field with a von Kármán energy spectrum. He found that for an eighth-order finite difference scheme, the LES filter size must be at least twice the grid spacing for the contribution of the SFS force to the total nonlinear force to be significant compared to the errors introduced by aliasing and truncation. For a second-order finite difference scheme, Ghosal found that the filter must be at least four times the grid spacing. Kravchenko and Moin [5] performed a posteriori tests which indicated that different (but analytically equivalent) formulations of the nonlinear terms give different results because of finite difference and aliasing errors. Blaisdell et al. [2] present results which indicate that choosing a particular form for the nonlinear terms with finite differencing may stabilize the results and reduce the need for dealiasing. There have also recently been several studies which have developed improved higher-order finite difference schemes with the aim of reducing numerical errors in LES (see for example [1,8]). Others have performed studies which have explicitly investigated numerical errors with regard to LES or specifically the computation of SFS models (see [4,9,11]).

Here we present results from error analysis performed using a direct numerical simulation dataset to generate a filtered subset representing "exact" LES data. In particular, we aim to examine the conclusions of Ghosal [3] with a more realistic flow field. As his results from von Kármán spectra have not been verified by analysis of real datasets, we seek to re-evaluate his conclusions here, commenting on differences due to the nature of the data used. As most LES calculations of engineering interest are performed at moderate Reynolds numbers, we expect the DNS dataset to be informative. Consideration of SFS model performance in relation to numerical errors is not the focus of this work and will not be addressed.

In Section 2 we describe the dataset and our approach in the a priori testing. Following, in Section 3, we discuss the relative magnitudes of the SFS force and nonlinear terms in relation to filter size and resolution. Sections 4 and 5 discuss finite difference and aliasing errors, and compare them to an ideal SFS forcing term.

2. Numerical tests

The DNS data used for a priori testing are from the stably stratified homogeneous shear flow simulations performed by Shih et al. [10]. The Reynolds number based on the Taylor microscale is 89.44, the Richardson number is 0.16, and the nondimensional shear number is 2.0. This dataset were chosen because it is homogeneous (allowing use of Fourier analysis) but has the increased complexity generated by the stratification; turbulent length scales are reduced due to the stratification and therefore are more difficult to model than those from a flow with neutral stratification. We expect that the results from this dataset will be more realistic than those of a simpler homogeneous flow, however we have also examined an isotropic turbulence case produced by the same DNS code and found similar results. The results from this analysis should therefore be appropriate for extension to moderate Reynolds number flows.

The velocity fields used for a priori testing are obtained by using a sharp Fourier cutoff filter on the full 128^3 DNS data. These cutoff filtered fields are treated as "exact" data for a given grid size. Thus, u_i for a particular grid size is obtained by cutoff filtering the DNS data to remove the high wavenumbers which would not be present on a coarser grid. LES quantities such as $\overline{u}_i$ and $\overline{u_i u_j}$ are then obtained for each grid

size using a Gaussian filter in spectral space. We choose not to use a spectral cutoff filter for calculation of these LES variables since our primary application area of interest is in complex geometries where finite difference methods are used. A tophat filter could also be used to give comparable results; the discrete filter coefficients used for tophat and Gaussian filters with finite difference methods are similar.

Fig. 1 shows the three-dimensional energy spectra for the velocity fields used to study numerical errors. Several grid cutoff wavenumbers are considered to study the effect of different grid resolutions; the grid is reduced from 128^3 for the original DNS to 64^3, 32^3, 16^3, and 8^3 for the LES grids. Using these "exact" fields, we can compute the nonlinear and SFS terms for LES using different methods and compare results for the magnitudes of errors. Notice that the shape of these spectra are quite different than the von Kármán energy spectra used by Ghosal [3]. In particular, due to the low Reynolds number of the DNS dataset, the inertial range is very small, as seen by comparison to the $-5/3$ slope also plotted. We therefore expect that our analysis of this dataset may yield different conclusions from the high Reynolds number results of Ghosal.

The energy spectra in Fig. 1 and in all the following figures are computed for spherical shells and plotted versus the magnitude of the wavenumber. The spherical wavenumber is computed as $\kappa = \sqrt{k_1^2 + k_2^2 + k_3^2}$, where k_1, k_2, and k_3 are the Cartesian wavenumbers. Energy from each wavenumber triplet k_1, k_2, and k_3 is assigned to the corresponding wavenumber bin for κ, chosen at the nearest integer level. The spectra are often not smooth at the highest wavenumbers due to inadequate statistical sampling in the outer spherical shells. However, the 1-D spectra (not shown) for these quantities are smooth even at the tail ends. For simplicity, we will refer to the grid size and the chosen filter–grid ratio (FGR) instead of the exact cutoff wavenumber for each LES grid. In addition, most results are presented for the case when the Gaussian LES filter width is twice the grid spacing (with a 32^3 grid). We use this as our base case as this ratio seems to be the most commonly used in the recent literature. We consider other filter widths in our analysis and comment on their effect. All numerical tests are performed in Fourier space, as described further in the sections that follow.

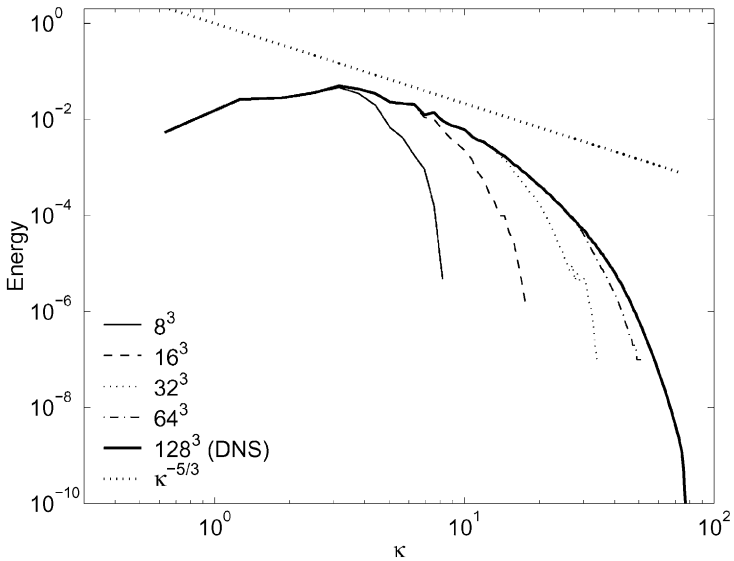

Fig. 1. Three-dimensional energy spectra of the "exact" velocity fields used for analysis, obtained by cutoff-filtering the original DNS dataset. A $\kappa^{-5/3}$ line is also plotted for comparison.

3. Comparison of total nonlinear and subfilter-scale terms

The full nonlinear term in the Navier–Stokes equations, $\partial u_i u_j/\partial x_j$, creates a closure problem in LES when this term is filtered: $\overline{\partial u_i u_j/\partial x_j}$. The usual approach in LES is to replace this term with the closed term $\partial \overline{u}_i \overline{u}_j/\partial x_j$ (assuming the filter and derivatives commute) and to subtract a SFS force term, $\partial \tau_{ij}/\partial x_j$, from the right-hand side of the equation, where $\tau_{ij} = \overline{u_i u_j} - \overline{u}_i \overline{u}_j$. This effectively transfers the closure problem to the right-hand side of the filtered Navier–Stokes equations. Traditionally the approach has been to model τ_{ij} as a purely dissipative term, using an eddy-viscosity formulation. Recent work has shown that this method may not be adequate, especially when the flow dynamics are sensitive to energy backscatter (counter-gradient transfer from small to large scales) in the flow.

It is interesting to compare the relative magnitudes of the SFS term, $\partial \tau_{ij}/\partial x_j$, and the total nonlinear term, $\partial \overline{u}_i \overline{u}_j/\partial x_j$. In an ideal LES, the sum of these terms is equal to the full nonlinear term $\overline{\partial u_i u_j/\partial x_j}$ which can be obtained from a DNS (after filtering). In practice, the contribution to the total nonlinear term depends on the SFS model used. However, even with a perfect SFS model, the contribution of the SFS model would depend on the filter size chosen. The larger the filter size, the more energy is placed in the subfilter scales, and the larger the SFS term must be. Fig. 2 shows the dependence of the SFS term on the filter size for a fixed grid resolution. This is similar to Fig. 2 in Ghosal's paper [3], however the spectra are quite different, as the spectrum of the nonlinear terms generated from the von Kármán spectrum increases monotonically while there is a definite downturn in the present data.

Another important trend is that as the resolution of the grids we consider increases (and hence the absolute filter width decreases for a given filter–grid ratio), the results approach that of a DNS. Thus the relative contribution of the SFS term to the total nonlinear term (at a fixed filter–grid ratio) becomes smaller as resolution is increased. This trend can be seen in Fig. 3 where a global measure of the nonlinear and SFS terms is plotted for different grid resolutions. The values are normalized (unlike Ghosal's Fig. 6) by the total for both the nonlinear and SFS terms, since the totals are dependent on the grid resolution. The

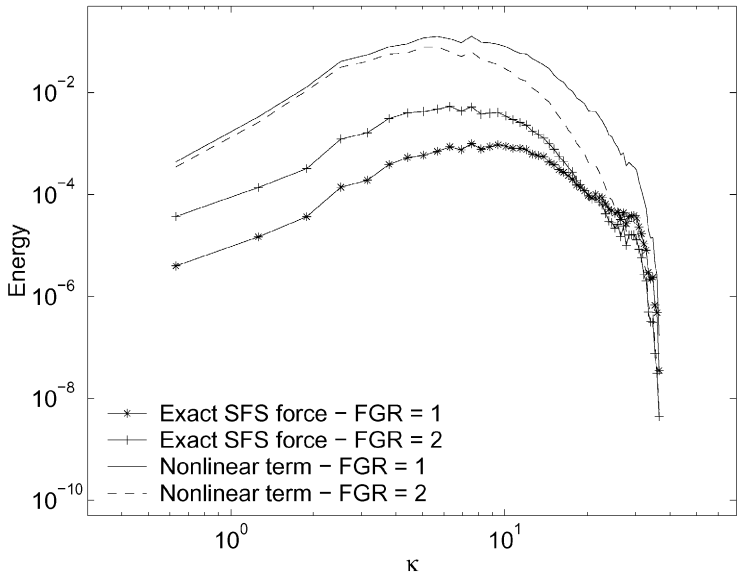

Fig. 2. Energy spectra of the spectrally computed (filtered) nonlinear term (in the dealiased divergence form) and the SFS term for a fixed resolution (32^3 grid) and filter–grid ratios of one and two.

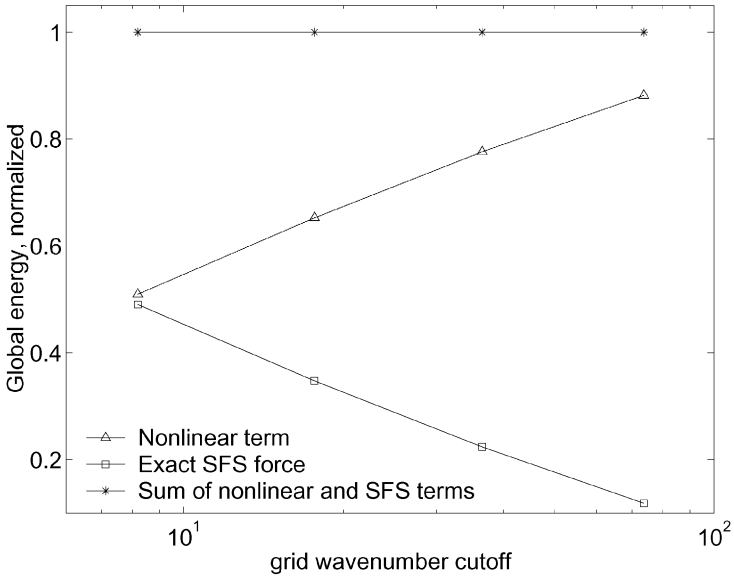

Fig. 3. Global energies of the spectrally computed nonlinear term (in the dealiased divergence form) and the SFS term for different grid resolutions, normalized by the sum of the nonlinear and SFS terms. Data points are shown at the 8^3, 16^3, 32^3, and 64^3 grid resolution locations. Filter–grid ratio = 2.

global measure is the same as that in Ghosal's equation (81), which is the square root of the integral of the energy spectrum:

$$\sigma_* = \left[\int_0^{\kappa_m} E^{(*)}(\kappa)\, d\kappa \right]^{1/2}. \tag{1}$$

Here σ_* is the global measure for a particular quantity (such as the nonlinear terms, error terms, etc.), $E^{(*)}$ is the three-dimensional energy spectrum for that quantity, and κ_m is the maximum wavenumber magnitude. Note that in our case the power spectrum includes the corners of the wave space, unlike Ghosal's.

Thus, the importance of accurately representing the SFS term is greatest at low resolutions where the SFS term contributes a larger percentage of the total force. However, at low resolutions, numerical error also becomes more significant because fine-scale motions are not well-represented on the grid.

4. Finite differencing errors

Modified wavenumber analysis is useful for examining truncation errors of different numerical schemes. The modified wavenumber, k', for a finite difference scheme, is derived by discrete differentiation of $u = \exp(ikx)$ [7]. Finite difference schemes exhibit large errors near the grid wavenumber cutoff, as evidenced by the reduced magnitude of the modified wavenumbers. Higher-order finite difference methods perform better; however all finite difference methods have low modified wavenumbers near the grid cutoff point. To examine the effect of truncation errors, we will insert the modified wavenumbers in place of the true wavenumber into spectral differentiation routines to compare finite difference and spectral results, as was done by Kravchenko and Moin [5].

Even though all spatial derivatives in the LES equations will have finite differencing errors, we are primarily interested in the truncation error in the nonlinear term because this has the potential to be very

large and overshadow the contribution of the SFS term. In Fig. 4 we compare the spectrum of the finite difference error in computing the nonlinear term (computed using the divergence form defined later in Eq. (3)) to the SFS force term, with a filter–grid ratio of unity. The finite difference error is computed by subtracting the nonlinear term calculated with a finite difference scheme from that of the exact (spectrally calculated) nonlinear term. We see that the trend is similar to that in Ghosal's Fig. 4: the SFS force at high wavenumbers is dominated by the error in the nonlinear terms, even when the nonlinear terms are computed with a sixth-order Padé scheme.

This situation cannot be improved by increasing the grid resolution, as also demonstrated by Ghosal (see his Fig. 3) [3]. When the grid resolution is increased, finer-scale motions are better resolved and the role of the SFS term decreases, as seen in Fig. 3. The finite difference error does not decrease, however, as the grid must now resolve a larger range of motions as these are no longer in the subfilter range. Thus the finite difference error continues to dominate the SFS term.

Ghosal [3] suggests that by choosing the proper filter–grid ratio (FGR) in combination with a high-order finite difference scheme it is possible to reduce the finite difference error sufficiently. He shows that the filter–grid ratio has a pronounced effect on the magnitude of the error term. We observe the same trend when this is done for our DNS dataset. However, we choose to make the comparisons differently. Instead of keeping the filter cutoff fixed and changing the grid size as Ghosal does, we keep the grid size fixed and change the filter size to change the filter–grid ratio. Though the trends observed are similar, our perspective is more directly applicable to real LES computations: the grid resolution is not readily increased because of computer limitations, but the filter–grid ratio can be adjusted easily.

Fig. 5 shows that increasing the filter–grid ratio by a factor of two improves results appreciably. The errors for the second-order and fourth-order finite difference schemes and the Padé scheme are smaller over much of the wavenumber range, though the errors still dominate at high wavenumbers. This is consistent with Ghosal's conclusions. In particular we see similar features in our Fig. 5 and Ghosal's Fig. 10, for a filter–grid ratio of two. It is not until the filter–grid ratio is equal to four that the second-order finite difference scheme becomes acceptable. Fig. 6 shows the results for this combination, where the truncation

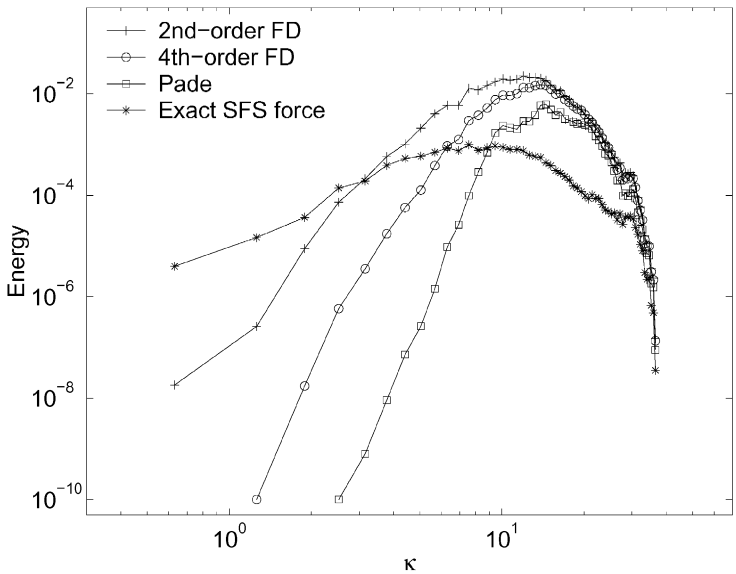

Fig. 4. Energy spectra of the finite differencing error in the nonlinear term in the dealiased divergence form, computed with second- and fourth-order finite difference (FD) and sixth-order Padé schemes, compared to the SFS force term. Filter–grid ratio = 1; 32^3 grid.

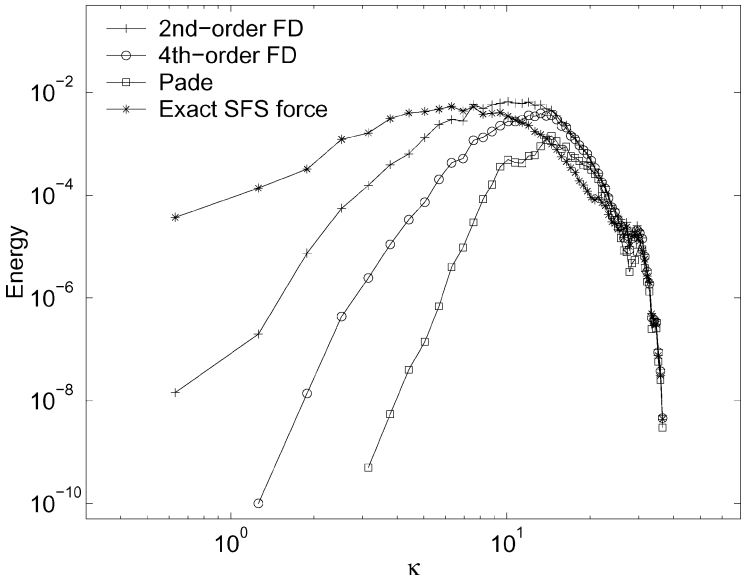

Fig. 5. Energy spectra of the finite differencing error in the nonlinear term in the dealiased divergence form, computed with second- and fourth-order finite difference and sixth-order Padé schemes, compared to the SFS force term. Filter–grid ratio = 2; 32^3 grid.

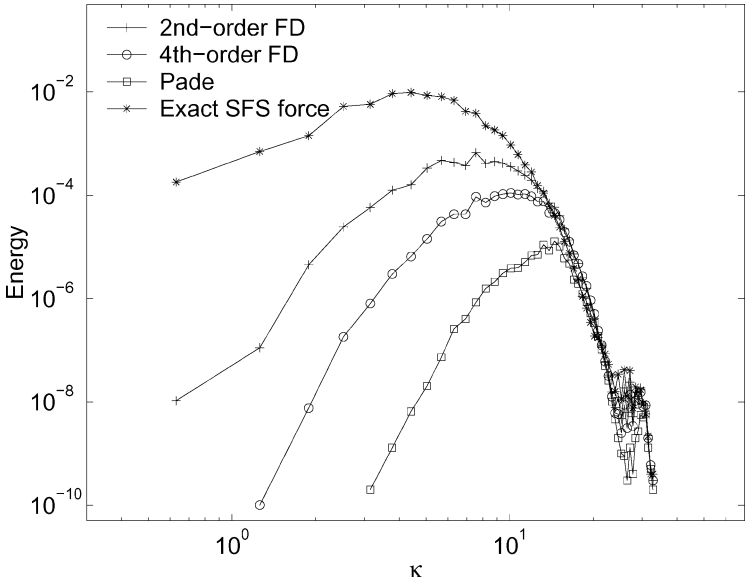

Fig. 6. Energy spectra of the finite differencing error in the nonlinear term in the dealiased divergence form, computed with second- and fourth-order finite difference and sixth-order Padé schemes, compared to the SFS force term. Filter–grid ratio = 4; 32^3 grid.

error no longer dominates the SFS force. Ghosal's Fig. 9 also indicates that for a second-order central difference scheme, the filter–grid ratio should be at least 4, which is consistent with our results, even though his plot is for a grid 4^3 times larger.

Fig. 7 shows the global truncation error compared to the global SFS force for a filter–grid ratio of two. The terms are normalized with respect to the total nonlinear terms to adjust for the energy at different grid resolutions. For a filter–grid ratio of two, only the Padé scheme gives a total error significantly less than the SFS force for all grid resolutions. Notice that the global SFS force is larger than all the errors for grid sizes of 8^3 ad 16^3, regardless of the scheme used. The explanation for this is probably that at such coarse resolution, the "exact" field we are comparing to (see Fig. 1) does not contain much energy or many fine scale motions, so the error from differentiation is not large since the field is smooth.

It is also important to understand exactly what the consequences are of adjusting the filter–grid ratio. When the filter size is increased on a fixed grid, a larger portion of motions must be represented by the SFS term. Fig. 8 shows the total errors for the second-order finite difference scheme for different grid resolutions and filter–grid ratios. This verifies our conclusion from Figs. 4–6 that increasing the filter–grid ratio makes the total finite differencing error much smaller. Fig. 8 indicates that for all grid resolutions, error is reduced by increasing the filter–grid ratio. The magnitude of the SFS force increases with the filter–grid ratio, as more of the energy is placed into the subfilter scales, so that for FGR = 4 the SFS force dominates the error for all grid resolutions.

In summary, Ghosal's results lead to the conclusion that if the effect of the SFS terms is to be significant, it is necessary to compute SFS terms using a filter width that is at least twice the size of the grid spacing, and then only with an eighth-order finite difference scheme. To achieve the same results with a second-order scheme, the filter would have to be made at least four times larger than the grid spacing. In our tests (which use realistic spectra for low Reynolds number flows), we find that the sixth-order Padé scheme performs very well for FGR = 2 or greater. If a second-order scheme is to be used, FGR = 4 will give a global finite difference error that is smaller than the SFS term. These requirements are quite stringent. In practice, many LES codes use second-order finite difference methods with a filter–grid ratio of unity or at best two. Some of the results of these LES codes are likely contaminated by significant numerical errors.

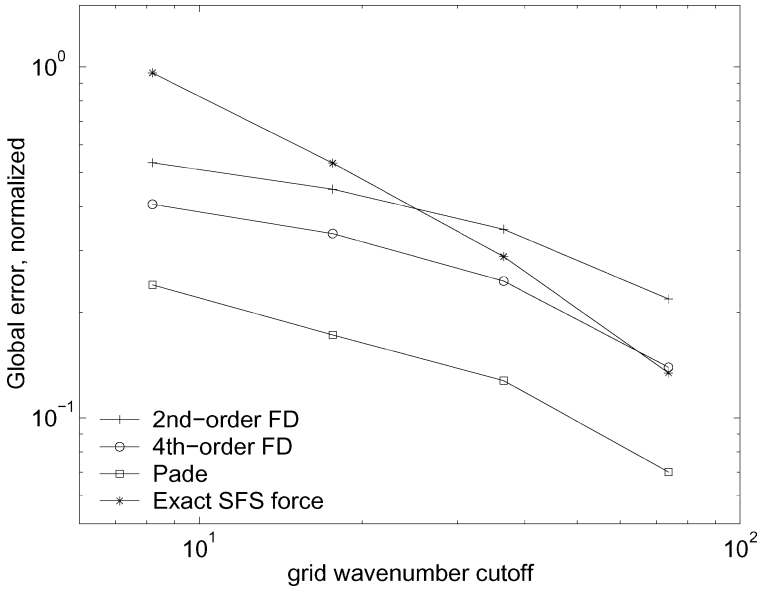

Fig. 7. Global finite differencing error in the nonlinear term in the dealiased divergence form, computed with second- and fourth-order finite difference and sixth-order Padé schemes, compared to the SFS force term. Data points are normalized by the total nonlinear terms and shown at the 8^3, 16^3, 32^3, and 64^3 grid resolution locations. Filter–grid ratio = 2.

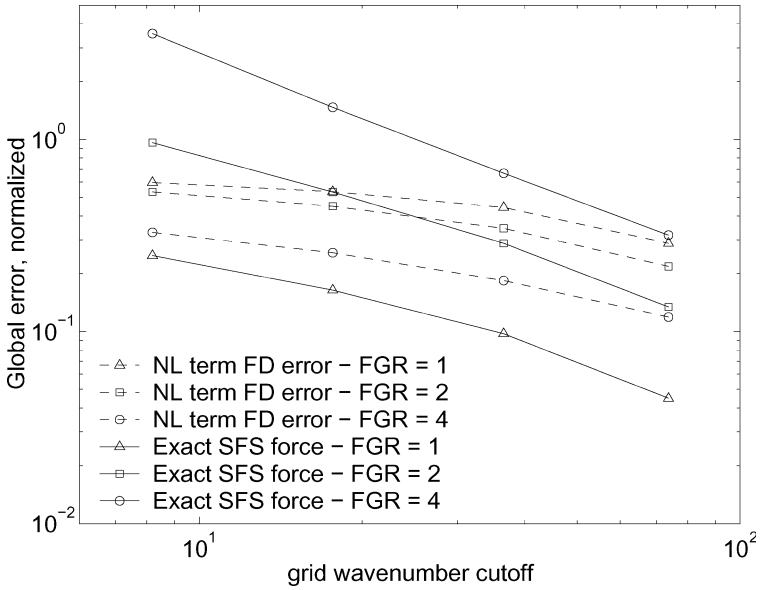

Fig. 8. Global finite differencing error in the nonlinear term (NL) in the dealiased divergence form, for second-order finite differencing, compared to the SFS force term for different filter–grid ratios. Data points are normalized by the total nonlinear terms and shown at the 8^3, 16^3, 32^3, and 64^3 grid resolution locations.

5. Aliasing errors

Aliasing errors occur when variables are multiplied in physical space; high frequency components produce higher frequency components which cannot be adequately represented on a finite grid. Thus, the frequencies beyond the grid wavenumber cutoff are incorrectly "aliased" to wavenumbers that are resolved [7]. The contribution of aliasing errors is largest at the highest wavenumbers where any energy above the wavenumber cutoff incorrectly "folds over" into the resolved spectrum. While these aliasing errors appear to be important only at high wavenumbers, it is of interest to compare them to the SFS force term. Aliasing errors prevent a numerical method from conserving energy and hence can cause the solution to be unstable, as shown by Kravchenko and Moin [5]. Aliasing errors can be removed, but this is computationally expensive, even in spectral codes where the 3/2-rule for dealiasing is applicable and is relatively straightforward to implement. Lele suggests a filtering method for dealiasing in physical space though this method also requires extra computation [6]. Because of this cost and the difficulty of implementation in non-spectral codes, dealiasing is not often performed in finite difference codes, even though these are also affected by aliasing errors. Neglecting to dealias product terms may be acceptable in finite difference codes, however, because the effect of aliasing on the total error may be somewhat reduced in finite difference schemes, as shown below. We will compare aliasing errors in the nonlinear term to the SFS forcing, and examine the error when finite difference schemes are used.

Fig. 9 compares spectra of the aliasing error incurred in computing the nonlinear terms to the SFS force. The error is defined as the difference between the aliased and dealiased calculations for a particular differencing scheme. Dealiasing is performed using the 3/2-rule in the spectral space calculations. Errors are the largest for the spectral scheme. For finite difference schemes, aliasing is reduced because the modified wavenumbers for finite difference methods decrease near the cutoff wavenumber. Finite differencing errors reduce the amount of aliasing error present, however they lead to a less accurate representation of the nonlinear terms at higher wavenumbers, as seen in the previous section.

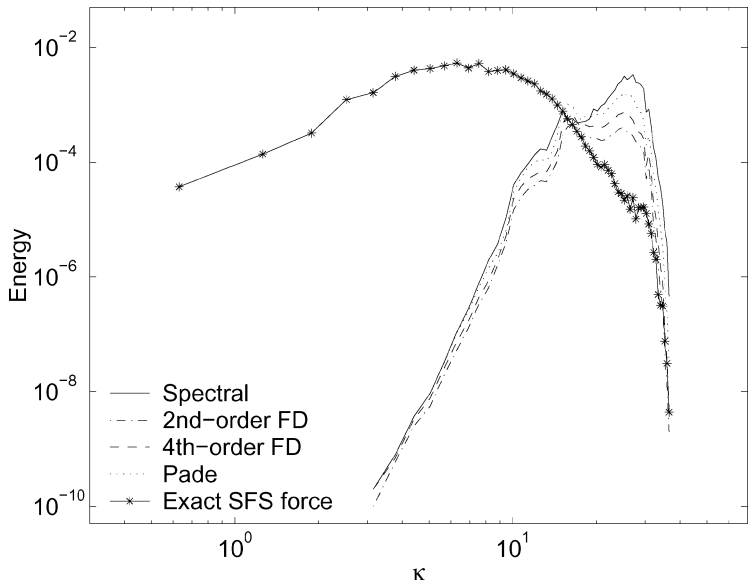

Fig. 9. Energy spectra of the aliasing error in the nonlinear term in the divergence form, computed with spectral, second- and fourth-order finite difference, and sixth-order Padé schemes, compared to the SFS force term. Filter–grid ratio = 2; 32^3 grid.

These results are consistent with Ghosal's [3], however the shape and magnitude of the spectra are quite different. Fig. 9 shows that for FGR = 2 the errors are larger than the SFS term only at high wavenumbers, as opposed to Ghosal's Fig. 5 where the aliasing error dominates in the entire range (for FGR = 1). In addition, in Ghosal's data the aliasing errors are more severe than the finite difference errors. In our case, the aliasing errors are significantly smaller than the finite difference errors for FGR = 2. By comparing Fig. 10 for aliasing errors to Fig. 7 for finite difference errors, we see that the global SFS force dominates the global aliasing error for all grid resolutions. This difference between our results and Ghosal's may be due to the nature of the dataset used. Even though the total aliasing error is less than the SFS force, aliasing errors can have an adverse affect on the numerical solution because they are concentrated at high wavenumbers. It is also in this high wavenumber range that SFS models may act to extract information to model the subfilter scales.

Like finite difference errors, aliasing errors can be reduced by increasing the filter–grid ratio, as product terms are more accurately represented on the grid when the original field is relatively smooth. The total aliasing errors for different grid sizes and different filter–grid ratios are plotted in Fig. 11, with aliasing error computed for the spectral differencing case and the divergence form of the nonlinear force. The total aliasing error decreases with increasing filter–grid ratio, as more of the motions are smoothed out and product terms are more accurately represented on the grid. For FGR = 2 and 4, the total SFS force is larger than the aliasing errors; however for FGR = 1, the aliasing error dominates, and is comparable in magnitude to the finite difference error in Fig. 8.

In addition to the effects of the finite difference scheme and the filter–grid ratio on the aliasing error, Blaisdell et al. [2] show that the form of the nonlinear terms can affect aliasing, so that proper choice of the discrete representation of these terms can reduce aliasing without any removal schemes. To further demonstrate the effect of aliasing error in the nonlinear terms, we evaluate the nonlinear terms using the rotational, divergence, convective, and skew-symmetric forms. These forms are analytically equivalent (see [5]):

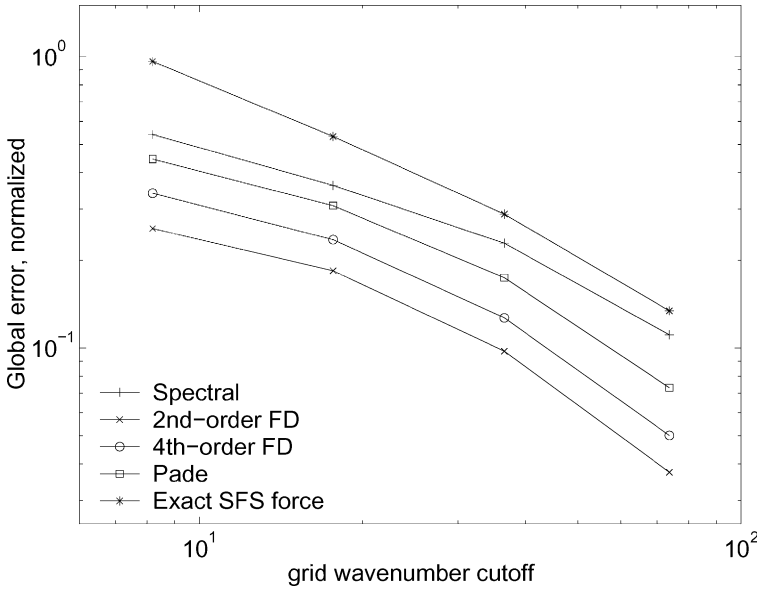

Fig. 10. Global aliasing error in the nonlinear term in the divergence form computed with spectral, second- and fourth-order finite difference, and sixth-order Padé schemes, compared to the SFS force term. Data points are normalized by the total nonlinear terms and shown at the 8^3, 16^3, 32^3, and 64^3 grid resolution locations. Filter–grid ratio = 2.

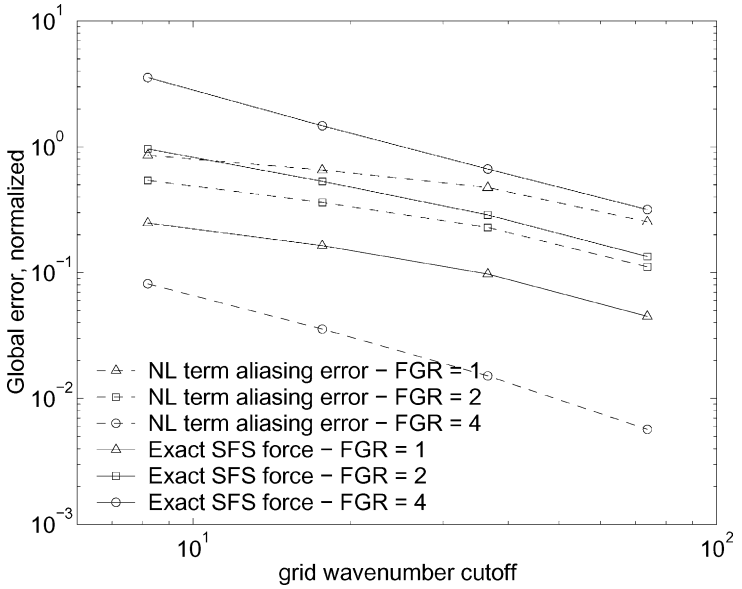

Fig. 11. Global aliasing error in the nonlinear term (NL) in the divergence form with spectral differencing, compared to the SFS force term for different filter–grid ratios. Data points are normalized by the total nonlinear terms and shown at the 8^3, 16^3, 32^3, and 64^3 grid resolution locations.

$$\text{Rotational}: \quad u_j\left(\frac{\partial u_i}{\partial x_j}-\frac{\partial u_j}{\partial x_i}\right)+\frac{1}{2}\frac{\partial u_j u_j}{\partial x_i}, \tag{2}$$

$$\text{Divergence}: \quad \frac{\partial u_i u_j}{\partial x_j}, \tag{3}$$

$$\text{Convective}: \quad u_j\frac{\partial u_i}{\partial x_j}, \tag{4}$$

$$\text{Skew-symmetric}: \quad \frac{1}{2}\left(\frac{\partial u_i u_j}{\partial x_j}+u_j\frac{\partial u_i}{\partial x_j}\right). \tag{5}$$

In discrete form, however, these expressions may not be equivalent, as this depends on whether the product rule for differentiation holds numerically.

For dealiased spectral methods, differentiation is exact and therefore satisfies the product rule, so the four formulations perform identically. The difference in the formulations without dealiasing can be significant, as seen in Fig. 12 for spectral schemes, which shows spurious energy at the highest wavenumbers. For finite difference schemes, even when all terms are dealiased the results are different because of truncation errors. When second-order finite differences are used, the differences between these formulations are reduced (not shown) from those in Fig. 12, but may still be significant for numerical stability, so it is desirable to choose a formulation that gives the least error.

Fig. 13 shows spectra of aliasing errors for the different nonlinear formulations, compared to the SFS force. The convective formulation gives the least aliasing error, followed by the skew-symmetric and di-

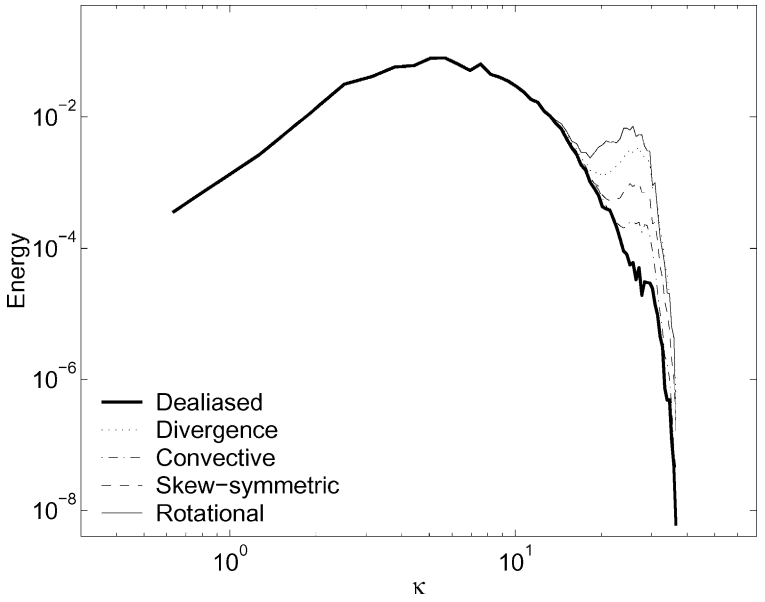

Fig. 12. Energy spectra of the nonlinear term with divergence, convective, skew-symmetric, and rotational formulations with derivatives computed spectrally, but aliasing error not removed. The dealiased spectrum is also shown. Filter–grid ratio = 2; 32^3 grid.

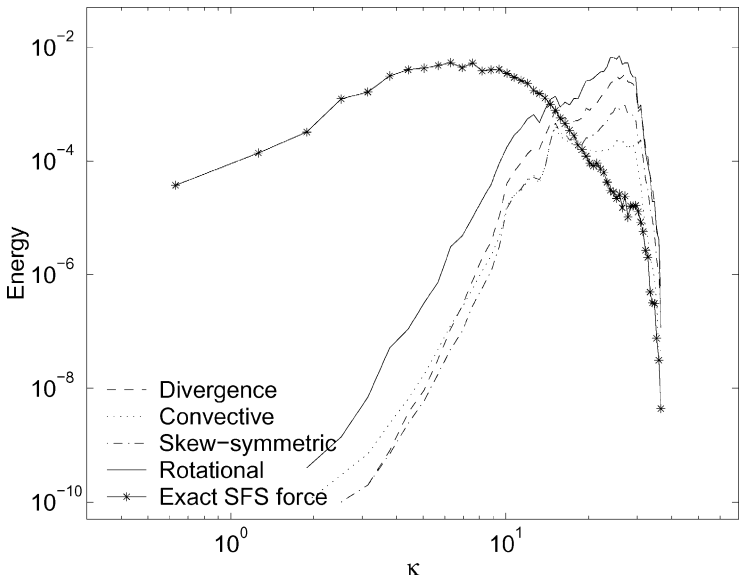

Fig. 13. Energy spectra of the aliasing error in the nonlinear term for the spectrally computed (but not dealiased) divergence, convective, skew-symmetric, and rotational formulations, compared to the SFS force term. Filter–grid ratio = 2; 32^3 grid.

vergence forms; the rotational form gives the highest error. These results are slightly different than those of the Fourier analysis of Blaisdell et al. [2] where the skew-symmetric form performs best, followed by the convective form. However, this is perhaps accounted for by the fact that their results are for compressible turbulence where the convective term consists of two parts; in incompressible flow this form reduces to one term because of the continuity condition. When directly implemented into a spectral LES code, Zang [12] and Blaisdell et al. [2] found the skew-symmetric form to be the preferred scheme because aliasing errors were minimized. Kravchenko and Moin [5] also found that the skew-symmetric form performed best in a finite difference code LES, while the convective form led to numerical instability which was linked to the sign of the truncation error. This poor performance of the convective form is not reflected in the spectra of errors shown here, indicating that a posteriori tests are needed to fully evaluate a particular scheme. We do, however, find that our error estimates are comparable to those of Zang [12], who found that the aliasing errors from the rotational form are about twice as large as those for the convection, divergence, and skew-symmetric forms. Fig. 14 shows the global error for different grid sizes using different nonlinear term formulations. For FGR = 2, the global errors from the rotational form are approximately two times larger than the errors from the other formulations and are comparable in magnitude to the total SFS terms.

Overall we observe a similar trend to Ghosal in analyzing the aliasing errors, however, the magnitude and shape of the spectra are different. In our case the aliasing error is concentrated at large wave numbers and does not dominate the SFS terms throughout the spectrum as long as the filter–grid ratio is greater than unity. Aliasing error is greatest for the higher-order finite difference schemes, and decreases with an increasing filter–grid ratio. For a non-dealiased finite difference code, it may be possible to use a particular formulation of the nonlinear terms to limit aliasing errors. It can be shown that aliasing errors of the two terms in the skew-symmetric form help to cancel each other out, so this form is often well-behaved even without dealiasing [5]. Blaisdell et al. [2] propose that the skew-symmetric version of the nonlinear terms eliminates most of the aliasing error, and hence provides a cheaper alternative to implementing a dealiasing scheme.

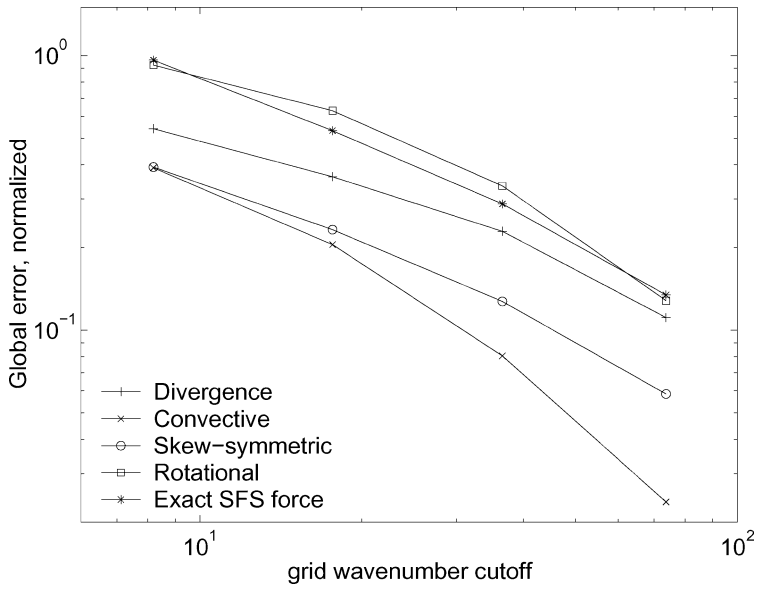

Fig. 14. Global aliasing error in the nonlinear term with divergence, convective, skew-symmetric, and rotational formulations (computed spectrally but not dealiased), compared to the SFS force term. Data points are normalized by the total nonlinear terms and shown at the 8^3, 16^3, 32^3, and 64^3 grid resolution locations. Filter–grid ratio = 2.

6. Conclusions

Following the approach of Ghosal [3], the analysis of DNS data presented here demonstrates some of the issues involved in the numerical representation of nonlinear terms and SFS terms. Results from our DNS dataset are similar to Ghosal's statistical analysis, confirming the need for careful selection of numerical parameters in LES. A few specific differences were noted.

To ensure that the SFS terms are larger than numerical errors from calculation of the nonlinear terms, the choice of the filter size is important. Our results indicate that the filter size should be at least twice as large as the grid spacing for a sixth-order Padé scheme. For a second-order finite difference scheme, the filter size should be at least four times the grid spacing. Because of the effect of the modified wavenumber, aliasing is less important for finite-difference methods than for spectral calculations; however, the representation at high wavenumbers with finite difference methods is less accurate because of the larger truncation errors. More accurate finite-difference methods can be used to represent the solution at higher wavenumbers better, but dealiasing or a particular discretization (e.g., the skew-symmetric form) of the nonlinear terms may then become necessary.

This study is a confirmation of Ghosal's results for high Reynolds numbers for flows at moderate Reynolds numbers. The above guidelines for LES are of course only directly applicable to moderate Reynolds number flows such as the one considered here. However, the general recommendations that require a specific filter–grid ratio to limit numerical errors in LES appear to apply to the entire range of Reynolds numbers, from low-to-moderate Reynolds number engineering flows to high Reynolds number geophysical flows.

Acknowledgements

One of the authors (F.K.C.) is supported by a National Defense Science and Engineering Graduate Fellowship and NSF Grant ATM-0073395 (Physical Meteorology Program: R.R. Rogers, Program Di-

rector). Thanks are due to Robert Street for his insightful comments on a draft of this manuscript, and to Lucinda Shih for providing the DNS data.

References

[1] D.S. Balsara, C.-W. Shu, Monotonicity preserving weighted essentially non-oscillatory schemes with increasingly high order of accuracy, Journal of Computational Physics 160 (2000) 405–452, doi:10.1006/jcph.2000.6443.
[2] G.A. Blaisdell, E.T. Spyropoulos, J.H. Qin, The effect of the formulation of nonlinear terms on aliasing errors in spectral methods, Applied Numerical Mathematics 21 (3) (1996) 207–219.
[3] S. Ghosal, An analysis of numerical errors in large-eddy simulations of turbulence, Journal of Computational Physics 125 (1996) 187–206, doi:10.1006/jcph.1996.0088.
[4] J.W. Glendening, T. Haack, Influence of advection differencing error upon large-eddy simulation accuracy, Boundary Layer Meteorology 98 (1) (2001) 127–153.
[5] A.G. Kravchenko, P. Moin, On the effect of numerical errors in large eddy simulations of turbulent flows, Journal of Computational Physics 131 (2) (1997) 310–322, doi:10.1006/jcph.1996.5597.
[6] S.K. Lele, Compact finite difference schemes with spectral-like resolution, Journal of Computational Physics 103 (1992) 16–42.
[7] P. Moin, Fundamentals of Engineering Numerical Analysis, Cambridge University Press, Cambridge, 2001.
[8] Y. Morinishi, T.S. Lund, O.V. Vasilyev, P. Moin, Fully conservative higher order finite difference schemes for incompressible flow, Journal of Computational Physics 143 (1998) 90–124, doi:10.1006/jcph.1998.5962.
[9] Y. Morinishi, O. Vasilyev, Subgrid scale modeling taking the numerical error into consideration, Annual Research Briefs, Center for Turbulence Research, NASA Ames-Stanford University, 1998.
[10] L.H. Shih, J.R. Koseff, J.H. Ferziger, C.R. Rehmann, Scaling and parameterization of stratified homogeneous turbulent shear flow, Journal of Fluid Mechanics 412 (2000) 1–20.
[11] M. Tsubokura, Proper representation of the subgrid-scale eddy viscosity for the dynamic procedure in large eddy simulation using finite difference method, Physics of Fluids 13 (2) (2001) 500–504.
[12] T. Zang, On the rotation and skew-symmetric forms for incompressible flow simulations, Applied Numerical Mathematics 7 (1991) 27–40.